HHS Public Access

Author manuscript

Nature. Author manuscript; available in PMC 2013 July 24.

Published in final edited form as:

Nature. 2013 January 24; 493(7433): 557–560. doi:10.1038/nature11716.

RNAi triggered by specialized machinery silences developmental genes and retrotransposons

Soichiro Yamanaka[1], **Sameet Mehta**[1], **Francisca E. Reyes-Turcu**[1], **Fanglei Zhuang**[2], **Ryan T. Fuchs**[2], **Yikang Rong**[1], **Gregory B. Robb**[2], and **Shiv I. S. Grewal**[1]

[1]Laboratory of Biochemistry and Molecular Biology, National Cancer Institute, National Institutes of Health, Bethesda, MD 20892

[2]New England Biolabs, Ipswich, MA 01938

Abstract

RNAi is a conserved mechanism in which small interfering RNAs (siRNAs) guide the degradation of cognate RNAs, but also promote heterochromatin assembly at repetitive DNA elements such as centromeric repeats[1,2]. However, the full extent of RNAi functions and its endogenous targets have not been explored. Here we show that in the fission yeast *Schizosaccharomyces pombe*, RNAi and heterochromatin factors cooperate to silence diverse loci, including sexual differentiation genes, genes encoding transmembrane proteins, and retrotransposons that are also targeted by the exosome RNA degradation machinery. In the absence of the exosome, transcripts are processed preferentially by the RNAi machinery, revealing siRNA clusters and corresponding increase in heterochromatin modifications across large domains containing genes and retrotransposons. We show that the generation of siRNAs and heterochromatin assembly by RNAi is triggered by a mechanism involving the canonical poly(A) polymerase Pla1 and an associated RNA surveillance factor Red1, which also activate the exosome. Remarkably, siRNA production and heterochromatin modifications at these target loci are regulated by environmental growth conditions, and by developmental signals that induce gene expression during sexual differentiation. Our analyses uncover interplay between RNAi and the exosome that is conserved in higher eukaryotes, and show that differentiation signals modulate RNAi silencing to regulate developmental genes.

In *S. pombe*, centromeric transcripts are processed by RNAi factors including Argonaute (Ago1)-containing RNA-induced transcriptional silencing (RITS) complex, RNA-dependent

Correspondence and requests for materials should be addressed to S.I.S.G (grewals@mail.nih.gov).

Supplementary Information is linked to the online version of the paper at www.nature.com/nature.

Author Contributions S.Y. and S.I.S.G. designed the experiments. F.Z., R.Y.T. S.Y. and G.B.R. prepared the library of small RNA for deep sequencing. S.M. processed the deep-sequencing data. S.Y., S.M. and S.I.S.G. analyzed the data. F.E.R.T and S.Y. carried out ChIP-chip. Y.R. performed the *Drosophila* genetic crosses. S.Y. performed all other experiments, if not stated. S.I.S.G. wrote the paper with input from all of the authors.

Author Information Microarray data are available at the NCBI Gene Expression Omnibus (GEO) repository under the accession number GSE41643. Reprints and permissions information is available at www.nature.com/reprints. The authors declare no competing financial interests.

RNA polymerase (Rdp1), and Dicer (Dcr1)[2]. Processing of transcripts into siRNAs is coupled to loading of Clr4/Suv39 required for histone H3 lysine 9 methylation (H3K9me)[3,4]. While most siRNAs correspond to centromeric repeats[5,6], siRNAs that match other repetitive structures such as *Tf2* retrotransposons have not previously been detected.

The 3′-5′ exonuclease activity of the exosome that also processes heterochromatic transcripts[7–9] acts in an overlapping manner to RNAi to silence centromeric transcripts[10], suggesting that RNAi and the exosome share targets. Recent studies have revealed widespread transcription of the genome[7,11,12], producing transcripts that are regulated by the exosome[7]. Under specific growth or developmental conditions, some of these transcripts may also feed into the RNAi pathway to generate siRNAs for heterochromatin assembly. Such RNAi targets might be detected in an exosome mutant, in which transcripts would be processed preferentially by RNAi machinery.

We performed high-throughput sequencing of small RNAs in cells lacking the exosome subunit Rrp6 to identify RNAi targets throughout the genome. We observed small RNA clusters mapping to various genomic locations. Equal densities of small RNA reads match forward and reverse strands of specific loci, and are abolished in RNAi mutants (Supplementary Table 1 and Figs. 1, 2). Overlapping transcription at convergent genes could induce RNAi[13], but siRNA clusters are also observed at non-convergent loci, suggesting an alternative mechanism.

Novel RNAi targets include loci in subtelomeric regions as well as protein coding genes, and siRNA clusters correlate with H3K9me enrichment (Supplementary Fig. 1 and Table 1). H3K9me peaks are dependent on RNAi (Figs. 1 and 2), and are distinct from heterochromatin islands that can be assembled without RNAi[14]. Closer examination of heterochromatin domains (HOODs) formed by RNAi shows that H3K9me and siRNA clusters are preferentially targeted to genes upregulated during sexual differentiation, as well as genes encoding transmembrane proteins (Supplementary Table 1). Several siRNA clusters overlap ncRNA (Supplementary Table 1)[15], which could potentially trigger RNAi[16].

Small RNAs that map to genes are predominantly 20–24 nucleotides (Fig. 1a), consistent with RITS-associated siRNAs[5]. Indeed, RITS subunit Chp1 localized to these loci (Fig. 1b). Small RNA production also requires Ago1 (Fig. 1a). The remaining reads in *ago1*Δ *rrp6*Δ display a broad length distribution consistent with degradation products (Supplementary Fig. 2). Ago1-dependent production of siRNA from *myp2* and *SPCC1442.04c* was confirmed by Northern blot (Fig. 1c), and is required for H3K9me at these loci (Fig. 1d and Supplementary Fig. 3a). In *rrp6*$^{+}$ cells, loss of Ago1, Dcr1, Rdp1 or Clr4 stabilized antisense transcripts from *myp2* and *SPCC1442.04c* (Fig. 1e), implicating RNAi and Clr4 in the regulation of these loci in wild-type cells.

Retrotransposons are silenced by several mechanisms to ensure genome stability[17]. In *S. pombe*, CENP-B proteins and chromatin modifiers silence *Tf2* retrotransposons and their remnants[18,19]. RNAi mutants show mild *Tf2* derepression and siRNAs mapping to these loci have not been detected[20,21]. We observed siRNA clusters and H3K9me in *rrp6*Δ at *Tf2* (Fig.

2a, b and Supplementary Fig. 3b). Small RNAs that map to the antisense strand show a preference for uridine at the 5′ end and a length profile of 20–24 nucleotides, while a portion of those mapping to the sense strand are likely degradation products (Fig. 2c). H3K9me is restricted to the *Tf2* ORF except for *Tf2s* located in close proximity where H3K9me could be detected at intervening regions (Supplementary Fig. 4a). siRNA generation and H3K9me at *Tf2* requires Ago1 and Dcr1 (Fig. 2a, b, d and Supplementary Fig. 4a). RNAi is also required for H3K9me and siRNA clusters at other repetitive elements, including a tandemly duplicated membrane transporter gene flanked by *LTR*s (Supplementary Fig. 4b).

We next asked if Clr4 is required for generation of siRNAs in a manner similar to its role at centromeres[2]. Small RNA profiling of *rrp6*Δ *clr4*Δ revealed that Clr4 is essential for siRNA production at *Tf2* (Fig. 2e, f), genes (Supplementary Fig. 5 and Table 1), and regions with little or no H3K9me (Supplementary Fig. 6a, b). Loss of Rdp1, which requires Clr4 for chromatin association[2], also abolished siRNA clusters (Fig. 2e, f and Supplementary Fig. 5). Thus, heterochromatin and RNAi factors cooperate to generate siRNA clusters.

We also explored assembly of HOODs in wild-type *S. pombe* cells cultured under varied growth conditions experienced in the natural environment. HOODs were observed in cells grown in carbon-limiting conditions or at low temperature (Supplementary Fig. 7). In low glucose, cells showed elevated levels of H3K9me at several HOODs including *Tf2*, *SPBC2D10.04* and the meiotic *mcp5* gene (Supplementary Fig. 7a, 8). Importantly, generation of siRNAs and HOOD formation at these loci were impaired in *ago1*Δ (Supplementary Fig. 8). Thus, assembly of HOODs is regulated by growth conditions in wild-type cells.

We investigated the functional significance of RNAi and heterochromatin factors in silencing target loci. Cells lacking Clr4 or RNAi in combination with *rrp6*Δ showed severe defects in silencing of *Tf2* and sexual differentiation genes (e.g. *mug5*, *mcp3*, *mek1* and *SPCC1442.04c*), in contrast to mild or no defects in single mutants (Fig. 3 and Supplementary Fig. 6c). Transcript levels were higher when *rrp6*Δ was combined with RNAi mutants than when combined with *clr4*Δ (Fig. 3a). These data clearly show that both RNAi and the exosome are important to fully silence these target loci.

Targeting of centromeric repeats by RNAi confers epigenetic repression on surrounding loci[22,23]. We found that both RNAi and the exosome coordinate the silencing of multiple loci within HOODs (Fig. 3b–d). Importantly, deletion of *man1* caused loss of H3K9me and defective silencing of surrounding genes (Fig. 3c, d). This finding reveals that nucleation of heterochromatin at genes via RNAi can modulate expression of other genes in *cis*.

Several siRNA clusters map to known targets of the RNA surveillance factor Red1, which silences sexual differentiation genes, genes encoding transmembrane proteins, and *Tf2*[24]. Red1 interacts with the poly(A) polymerase Pla1 and degrades transcripts via a mechanism involving the poly(A)-binding protein Pab2 and the exosome[24–26]. Combining *rrp6*Δ with *red1*Δ, *pab2*Δ, or *pla1-37* caused a reduction in siRNAs and H3K9me at *Tf2* and most genes (Fig. 4a, b and Supplementary Figs. 1, 9–11 and Table 2). In contrast, loss of the RNA binding protein Mmi1 that directs the exosome and RNAi to certain meiotic loci[27] had no

impact on siRNAs and H3K9me at most HOODs, except for a few loci including *man1* (Supplementary Figs. 5, 10 and Table 2). Interestingly, defects in Pla1 or Pab2 caused a reduction of H3K9me and siRNA clusters at *SPCC1442.04c* and *ste6*, while *red1*Δ had little effect, (Fig. 4c). Therefore, Pla1 and Pab2 may represent core machinery that cooperates with other factors, as dictated by genomic contexts, to direct H3K9me by RNAi.

We asked if Pla1 channels transcripts into the exosome and RNAi pathways. Our analysis revealed increased stabilization of *Tf2* and gene transcripts in *pla1-37 rrp6*Δ, similar to *ago1*Δ *rrp6*Δ or *dcr1*Δ *rrp6*Δ (Fig. 4d). Together with previous findings[24,26], these results suggest that Pla1 and associated factors such as Red1 process RNAs that feed into the exosome and RNAi. Indeed, loss of both Rrp6 and Ago1 was required to abolish H3K9me at *mcp5*, while *red1*Δ single deletion eliminated heterochromatin modification at this locus (Supplementary Fig. 12).

Since many of the RNAi targets are developmentally regulated, we asked if assembly of HOODs might be likewise regulated. We induced sexual differentiation in nitrogen starved *mat1-M* cells through ectopic expression of *mat1-Pc*. While nitrogen starvation alone had no effect, *mat1-Pc* expression caused the loss of siRNAs and H3K9me at *myp2* and *SPCC1442.04c* (Fig. 4e). siRNAs that map to *Tf2* were still detected (Fig. 4f), indicating that developmental signals selectively target HOODs that contain genes activated during sexual differentiation.

Finally, we explored the connection between RNAi and the exosome in higher eukaryotes. Small RNA profiling of *Drosophila rrp6*$^{-/-}$ revealed an increase in reads that map to repeat elements, as compared with control *rrp6*$^{+/-}$ larvae (Supplementary Fig. 13a, b). These small RNAs are predominantly 25–28 nucleotides and frequently begin with uracil, similar to piRNAs (Supplementary Fig. 13c, d)[17]. The sense and antisense transcripts of retroelements are upregulated in *rrp6*$^{-/-}$ larvae (Supplementary Fig. 13e). An increase in small RNAs that correspond to piRNA clusters (such as *42AB*) was also observed (Supplementary Fig. 14), suggesting that RNAi processes repeat transcripts in the absence of the exosome.

Our analyses suggest that RNAi collaborates with heterochromatin factors to silence developmentally regulated loci and retrotransposons, which are also targeted by the exosome. While not all loci displaying siRNA clusters in *rrp6*Δ might be bona fide targets, RNAi regulates several of these loci in response to physiological conditions in wild-type cells. The exosome may modulate the level of transcripts and/or siRNAs that trigger RNAi in response to developmental and environmental signals. In this regard, RNAi serves as an adaptive response mechanism that reprograms the genome under specific growth conditions. RNAi is triggered at developmentally regulated loci by specialized machinery that includes Red1 and Pla1 (Fig. 4g). These factors redistribute during sexual differentiation[24], and may be targets of a signaling cascade that regulates siRNA production. Other poly(A) polymerases, including Mlo3-TRAMP (Trf4/Air2/Mtr4 polyadenylation) that also activates both the exosome and RNAi[7], may share targets with Pla1 and Red1. Indeed, Mlo3 and TRAMP are required for silencing *Tf2* and duplicated genes[7]. Future studies may reveal interplay between RNA processing activities required for gene silencing during development and for genome stability in *S. pombe* and higher eukaryotes.

METHODS SUMMARY

ChIPs were performed using H3K9me antibody (Abcam) as described previously[5]. The preparation of small RNA libraries is described in Full Methods. For detection of small RNAs by Northern, 10μg of small RNAs, purified using the mirVana miRNA isolation kit (Ambion), were resolved on a 15% denaturing gel, crosslinked to neutral nylon membranes (Amersham/Pharmacia) and detected using a ~50nt ^{32}P-labeled single stranded RNA probe.

Full Methods are available in the online version of the paper.

METHODS

Strains and media

Standard protocols were used for cell culture, sporulation and tetrad analysis. Deletion of endogenous *man1* was performed by PCR-based gene targeting with clonNAT resistant genes as selection markers. Since *pla1* gene is essential for growth, a partial loss of function mutant allele of *pla1* (*pla1-37*) (a gift from M. Yamamoto's lab) was used. Wild-type and mutant cells were grown at 30 °C or 32°C in either rich (YEA) or minimal media (EMM). For nitrogen starvation, cells were cultured in EMM medium lacking nitrogen source. Strains and oligonucleotides used in this study are listed in Supplementary Tables 3 and 4, respectively.

Small RNA library construction

Small RNA fractions <40 nt were prepared by gel purification from denaturing acrylamide gels, or by using flashPAGE™ fractionation (Life Technologies) according to the manufacturer's recommendation[28]. Small RNAs were treated with CIP for 1 hour at 37°C at a ratio of 1 unit of Calf Intestinal Alkaline Phosphatase (New England Biolabs Inc., Ipswich USA) per pmole of RNA to remove mono, di, and triphosphates. After phenol /chloroform/ isoamyl alcohol extraction and ethanol precipitation, 3′-adapters (5′-App TCG TAT GCC GTC TTC TGC TTG T NH_2-3′) were ligated overnight at 16°C under conditions that are insensitive to 2′-O-methylation of the terminal nucleotide[28] (50 mM Tris pH 7.5, 10 mM MgCl2, 1mM DTT, 12.5% PEG.) Typical ligations contained ~1–3 pmoles (~10–30 ng) of small RNA. Adapters were in molar excess of RNA, and reactions contained 200 units of T4 Rnl2 truncated enzyme and 20 units of murine RNase inhibitor in a total volume of 20 μl. 10μl of the 3′-ligated RNA was phosphorylated by adding 3 μl of water, 0.5 μl of T4 Rnl1 buffer and 0.5 μl (20 U) of murine RNase inhibitor, and 1 μl (10 units) of T4 PNK (NEB) followed by incubation at 37°C for 30 min. Final buffer composition for this reaction was 50 mM Tris pH 7.5, 10 mM $MgCl_2$, 1mM DTT, 8.25% PEG, 0.33 mM ATP in a 15 μl reaction volume. The kinase was inactivated and the reverse transcription primer was annealed by adding a twofold molar excess (compared to 3′-linker) of reverse transcription primer and water in a volume of 5 μl. The 20 μl mixture was heated to 75°C for 10 minutes, incubated at 37°C for 10 minutes, and then cooled to 25°C. 22.5 pmoles of 5′-adapters (5′ rGrUrUrCrArGrArGrUrUrCrUrArCrA rGrUrCrCrGrArCrGrArUrC-3′), 20 units of murine RNase inhibitor, and 20 units of T4 RNA ligase 1 were added directly to the 3′-ligations and annealed to small RNA in a total reaction volume of 24 μl. Ligation reactions were

incubated at 25°C for 1 hour. Half (12 μl) of the doubly ligated small RNA was reverse transcribed using AMV RTase following the manufacturer's instructions (NEB) for 30 min at 42°C. One third of the cDNA was PCR amplified for 6–12 cycles using the primers 5′-CAA GCA GAA GAC GGC ATA CG-s-A-3′, and 5′-AAT GAT ACG GCG ACC ACC GAC AGG TTC AGA GTT CTA CAG TCC G-s-A-3′ (where -s- denotes phosphorothioate linkage) using 2× LongAmp®Taq Mastermix (NEB). PCR reactions were separated by native 6% PAGE. Amplified DNA was visualized by UV transillumination using SybrGold nucleic acid stain (Life Technologies), and regions of the gel corresponding to RNA insert sizes of 18–40nt were excised, crushed, and eluted from the gel in TE pH 8 for >2hr with at 25 °C. Libraries were concentrated using QiaQuick® columns (Qiagen, Valencia, USA) and analyzed using DNA1000 chips and reagents on an Agilent 2100 BioAnalyzer (Agilent, Santa Clara, USA).

ChIP analysis

ChIP and ChIP-chip analyses were performed as described previously with antibodies against dimethylated H3K9 (Abcam)[5]. In brief, exponentially growing cells (5×10^8) were fixed in 3% paraformaldehyde and chromatin. For ChIP of Chp1, cells were subsequently crosslinked by treatment of cells with 10 mM dimethyl adipimidate. Cells were washed with PBS, resuspended in lysis buffer (50 mM HEPES/KOH, pH 7.5, 140 mM NaCl, 1 mM EDTA, 1% Triton X-100, 0.1% DOC) and homogenized with glass beads. Chromatin was sheared by sonication to fragments of 500–1,000 bp, precleared with protein A slurry and immunoprecipitated with 2–4 μg of antibody. Immunoprecipitated chromatin was recovered by incubation with protein A or protein G slurry, washed extensively and reverse crosslinked by incubation at 65 °C. Immunoprecipitated DNA and DNA isolated from WCE were analysed by multiplex PCR or subjected to microarray-based ChIP-chip analysis.

Northern blot analysis

Northern blot analysis was performed as described previously[29]. Total RNA was isolated from cells with MasterPure yeast RNA purification kit (Epicentre). 10μg total RNA was loaded into each lane. Total RNA was transferred from gels to a positively charged nylon membrane (BrightStar-Plus, Ambion) using a specific transfer buffer (NorthernMax transfer buffer, Ambion). The ^{32}P-labeled single stranded RNA probes were hybridized overnight to the membrane in ULTRAhyb buffer (Ambion).

Detection of small RNAs by Northern blot

For small RNA detection, short RNAs (<200nt) were purified with the mirVana miRNA isolation kit (Ambion). 10 μg of small RNA was resolved on a 15% denaturing acrylamide gel, followed by transfer to a neutral nylon membrane (Amersham/Pharmacia). Chemical cross-linking was performed as previously described[30]. Cross-linked membrane was probed with ^{32}P-labeled single stranded RNA probes (~50nt) corresponding to *Tf2*, *myp2*, or *SPCC1442.04c*.

RT-PCR

Strand specific RT-PCR was carried out as previously described[31]. DNase-treated total RNA (100ng), isolated with MasterPure yeast RNA purification kit (Epicentre), was reverse transcribed using the One-step RT-PCR kit (Qiagen).

Drosophila genetics

The *rrp6* alleles used were f007001, which is a piggybac insertion into the *rrp6* coding region and was a gift from Dr. Elisa Lei at NIH, and *Df(3R)Exel6172*, which is a chromosomal deletion of the *rrp6* region and was obtained from the Bloomington Stock Center. Homozygous *rrp6* mutants were generated by crossing heterozygous *rrp6* flies that contained a balancer chromosome with an actin-driven GFP marker gene. Homozygous larvae were identified by the lack of GFP fluorescence throughout the body. Heterozygous siblings were used as controls. Since $rrp6^{-/-}$ flies failed to grow beyond the L1 larval stage, we profiled small RNAs from the L1 larvae of $rrp6^{-/-}$ and $rrp6^{+/-}$ flies.

Small RNA-seq analysis

Small RNA was sequenced using Illumina sequencing platform. Analysis of deep-sequencing data was performed using the commercial program Novoalign (http://www.novocraft.com). Novoalign was used to strip the adaptor sequences from the reads, and align them with the reference genome assembly of either *S. pombe* (September 2007 release) or *D. melanogaster* (NCBI release 5_30, May 30, 2011). The output parameters were set to report all valid alignments for each read, and only mapped reads were used in further analysis. Python and R scripts were used to further analyze the aligned read data. Python scripts were used to compile information about genome mapping coverage that included the length and the genomic coordinates of each read, and to generate a count of the number of times each position in the genome was represented in the data set. The coverage count (the number of times a read in the data set was mapped to a given location in the genome) was normalized to per million mapped reads. For the analysis of repetitive regions in *D. melanogaster*, the mapped reads were processed through the open source program, RepeatMasker[32]. RepeatMasker revealed the identity and abundance of repeats in the small RNA data set, which were plotted using R.

Supplementary Material

Refer to Web version on PubMed Central for supplementary material.

Acknowledgments

We thank M. Zofall and K. Zhang for helpful contributions, J. Barrowman for editing the manuscript, M. Yamamoto for the *pla1-37* strain, E. Lei for the *Drosophila rrp6* mutant, B. Walker and M. Pineda for their help in sequencing, and Grewal lab members for discussions. This study utilized the Helix Systems and the Biowulf Linux cluster at the NIH. This work was supported by the Intramural Research Program of the National Institutes of Health, National Cancer Institute.

References

1. Matzke MA, Birchler JA. RNAi-mediated pathways in the nucleus. Nat Rev Genet. 2005; 6:24–35. [PubMed: 15630419]
2. Reyes-Turcu FE, Grewal SIS. Different means, same end-heterochromatin formation by RNAi and RNAi-independent RNA processing factors in fission yeast. Curr Opin Genet Dev. 2012; 22:156–163. [PubMed: 22243696]
3. Bayne EH, et al. Stc1: a critical link between RNAi and chromatin modification required for heterochromatin integrity. Cell. 2010; 140:666–677. [PubMed: 20211136]
4. Zhang K, Mosch K, Fischle W, Grewal SIS. Roles of the Clr4 methyltransferase complex in nucleation, spreading and maintenance of heterochromatin. Nat Struct Mol Biol. 2008; 15:381–388. [PubMed: 18345014]
5. Cam HP, et al. Comprehensive analysis of heterochromatin- and RNAi-mediated epigenetic control of the fission yeast genome. Nat Genet. 2005; 37:809–819. [PubMed: 15976807]
6. Djupedal I, et al. Analysis of small RNA in fission yeast; centromeric siRNAs are potentially generated through a structured RNA. EMBO J. 2009; 28:3832–3844. [PubMed: 19942857]
7. Zhang K, et al. Clr4/Suv39 and RNA quality control factors cooperate to trigger RNAi and suppress antisense RNA. Science. 2011; 331:1624–1627. [PubMed: 21436456]
8. Murakami H, et al. Ribonuclease activity of Dis3 is required for mitotic progression and provides a possible link between heterochromatin and kinetochore function. PLoS One. 2007; 2:e317. [PubMed: 17380189]
9. Buhler M, Haas W, Gygi SP, Moazed D. RNAi-dependent and -independent RNA turnover mechanisms contribute to heterochromatic gene silencing. Cell. 2007; 129:707–721. [PubMed: 17512405]
10. Reyes-Turcu FE, Zhang K, Zofall M, Chen E, Grewal SIS. Defects in RNA quality control factors reveal RNAi-independent nucleation of heterochromatin. Nat Struct Mol Biol. 2011; 18:1132–1138. [PubMed: 21892171]
11. Dutrow N, et al. Dynamic transcriptome of *Schizosaccharomyces pombe* shown by RNA-DNA hybrid mapping. Nat Genet. 2008; 40:977–986. [PubMed: 18641648]
12. Wilhelm BT, et al. Dynamic repertoire of a eukaryotic transcriptome surveyed at single-nucleotide resolution. Nature. 2008; 453:1239–1243. [PubMed: 18488015]
13. Gullerova M, Proudfoot NJ. Cohesin complex promotes transcriptional termination between convergent genes in *S. pombe*. Cell. 2008; 132:983–995. [PubMed: 18358811]
14. Zofall M, et al. RNA elimination machinery targeting meiotic mRNAs promotes facultative heterochromatin formation. Science. 2012; 335:96–100. [PubMed: 22144463]
15. Rhind N, et al. Comparative functional genomics of the fission yeasts. Science. 2011; 332:930–936. [PubMed: 21511999]
16. Bitton DA, et al. Programmed fluctuations in sense/antisense transcript ratios drive sexual differentiation in *S. pombe*. Mol Syst Biol. 2011; 7:559. [PubMed: 22186733]
17. Malone CD, Hannon GJ. Small RNAs as guardians of the genome. Cell. 2009; 136:656–668. [PubMed: 19239887]
18. Cam HP, Noma K, Ebina H, Levin HL, Grewal SIS. Host genome surveillance for retrotransposons by transposon-derived proteins. Nature. 2008; 451:431–436. [PubMed: 18094683]
19. Anderson HE, et al. The fission yeast HIRA histone chaperone is required for promoter silencing and the suppression of cryptic antisense transcripts. Mol Cell Biol. 2009; 29:5158–5167. [PubMed: 19620282]
20. Hansen KR, et al. Global effects on gene expression in fission yeast by silencing and RNA interference machineries. Mol Cell Biol. 2005; 25:590–601. [PubMed: 15632061]
21. Woolcock KJ, Gaidatzis D, Punga T, Buhler M. Dicer associates with chromatin to repress genome activity in *Schizosaccharomyces pombe*. Nat Struct Mol Biol. 2010; 18:94–99. [PubMed: 21151114]

22. Hall IM, et al. Establishment and maintenance of a heterochromatin domain. Science. 2002; 297:2232–2237. [PubMed: 12215653]
23. Partridge JF, Scott KS, Bannister AJ, Kouzarides T, Allshire RC. *cis*-acting DNA from fission yeast centromeres mediates histone H3 methylation and recruitment of silencing factors and cohesin to an ectopic site. Curr Biol. 2002; 12:1652–1660. [PubMed: 12361567]
24. Sugiyama T, Sugioka-Sugiyama R. Red1 promotes the elimination of meiosis-specific mRNAs in vegetatively growing fission yeast. EMBO J. 2011; 30:1027–1039. [PubMed: 21317872]
25. Lemay JF, et al. The nuclear poly(A)-binding protein interacts with the exosome to promote synthesis of noncoding small nucleolar RNAs. Mol Cell. 2010; 37:34–45. [PubMed: 20129053]
26. Yamanaka S, Yamashita A, Harigaya Y, Iwata R, Yamamoto M. Importance of polyadenylation in the selective elimination of meiotic mRNAs in growing *S. pombe* cells. EMBO J. 2010; 29:2173–2181. [PubMed: 20512112]
27. Hiriart E, et al. Mmi1 RNA surveillance machinery directs RNAi complex RITS to specific meiotic genes in fission yeast. EMBO J. 2012; 31:2296–2308. [PubMed: 22522705]
28. Munafo DB, Robb GB. Optimization of enzymatic reaction conditions for generating representative pools of cDNA from small RNA. RNA. 2010; 16:2537–2552. [PubMed: 20921270]
29. Zofall M, et al. Histone H2A. Z cooperates with RNAi and heterochromatin factors to suppress antisense RNAs. Nature. 2009; 461:419–422. [PubMed: 19693008]
30. Pall GS, Hamilton AJ. Improved northern blot method for enhanced detection of small RNA. Nat Protoc. 2008; 3:1077–1084. [PubMed: 18536652]
31. Volpe TA, et al. Regulation of heterochromatic silencing and histone H3 lysine-9 methylation by RNAi. Science. 2002; 297:1833–1837. [PubMed: 12193640]
32. Tarailo-Graovac M, Chen N. Using RepeatMasker to identify repetitive elements in genomic sequences. Curr Protoc Bioinformatics. 2009; Chapter 4(Unit 4):10. [PubMed: 19274634]

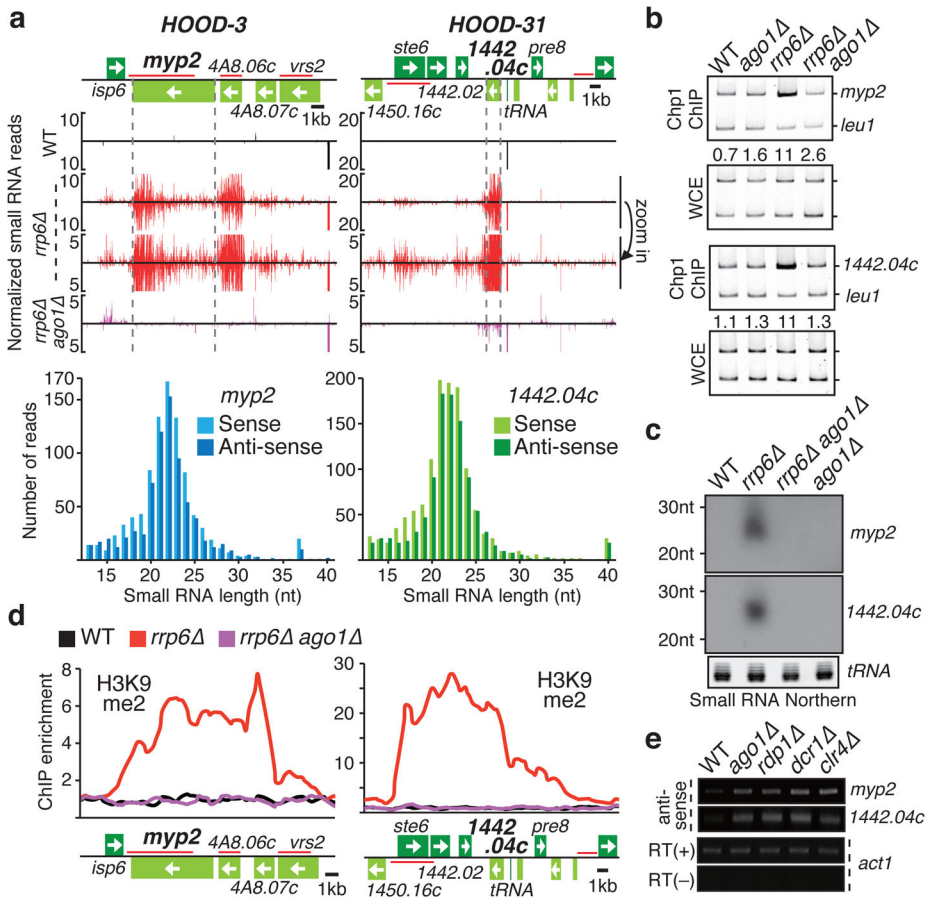

Figure 1. siRNA clusters and RNAi-dependent assembly of heterochromatin at gene-containing regions

a, The normalized number of small RNA reads are plotted. The signals above and below the line represent small RNAs that map to the top and bottom DNA strands, respectively. siRNA mapping to *myp2* and *SPCC1442.04c* and their length profiles are shown. **b**, Chromatin immunoprecipitation (ChIP) showing Chp1 enrichment at the indicated loci. The intensities of bands representing each locus and the *leu1* control in ChIP and whole cell crude extract (WCE) lanes were used to calculate the relative fold enrichments shown. **c**, Northern with probes specific for *myp2* or *SPCC1442.04c* was used to detect siRNAs. *tRNA* serves as a loading control. **d**, The H3K9me2 was mapped by ChIP-chip. siRNA clusters and H3K9me map to the open reading frames of multiple genes, but their distribution decreases sharply, in some cases coinciding with TFIIIC binding sites, such as *tRNAs*, that are known to serve as heterochromatin boundaries. **e**, Detection of antisense transcripts generated from *myp2* or *SPCC1442.04c* loci was performed using RT-PCR. The *act1* transcript level was used as a control.

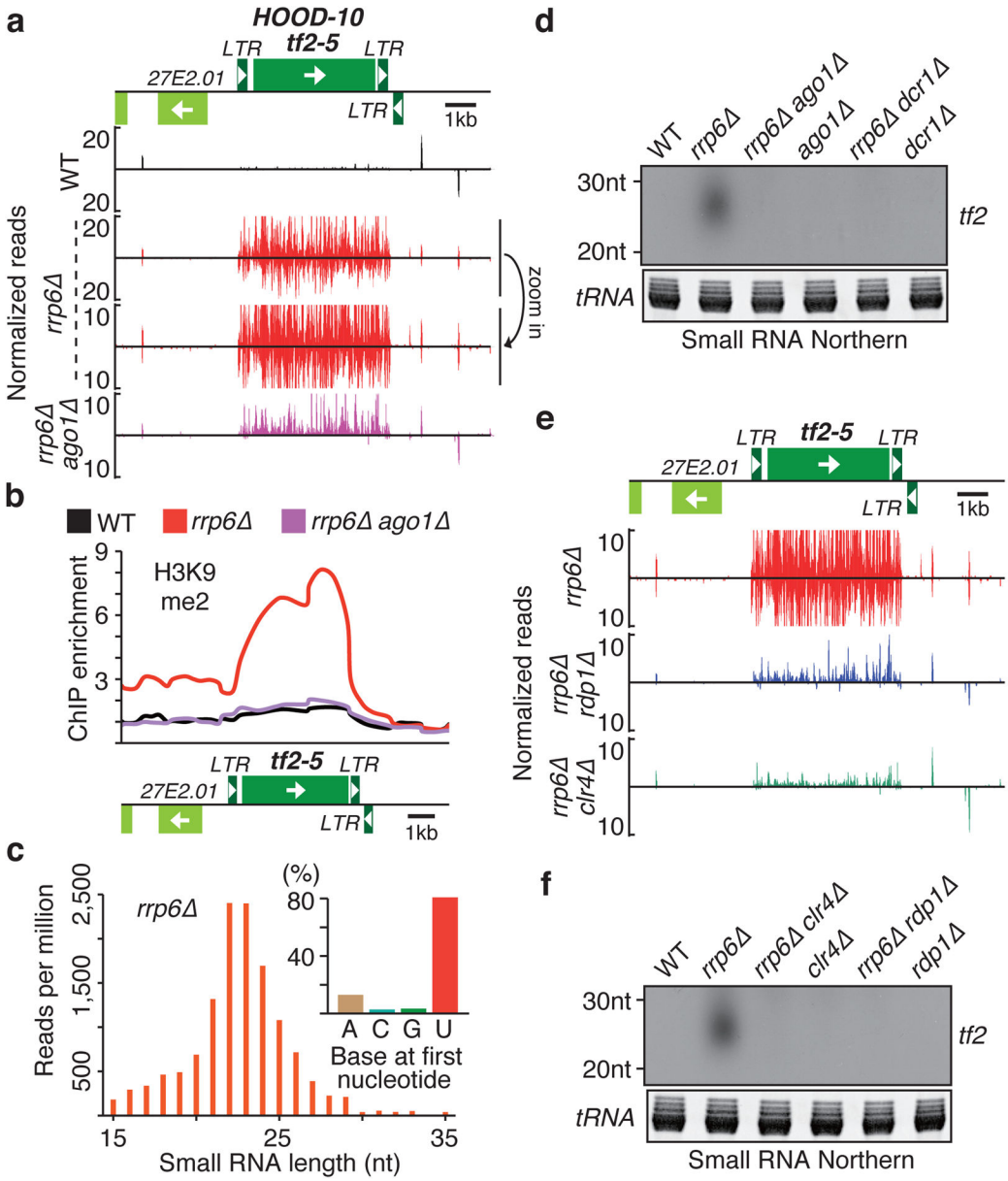

Figure 2. *Tf2* retrotransposons produce siRNAs and show RNAi-dependent heterochromatin formation

a, The small RNA reads that map to the region containing *Tf2*-5 in the indicated strains are plotted. **b**, The H3K9me2 distribution was determined by ChIP-chip. **c**, The length profile of small RNAs mapping to the antisense strand of *Tf2* is shown. The inset graph shows the frequency of the base at the 5′ end of reads that map to *Tf2*. **d**, Northern with probes specific for *Tf2* was used to detect siRNAs. *tRNA* serves as a loading control. **e**, Effects of Clr4 and Rdp1 on siRNAs mapping to *Tf2*. The small reads mapping to *Tf2*-5 in the indicated strains are plotted. **f**, Analysis of Clr4 and Rdp1 requirement for production of *Tf2* siRNAs. Results of the Northern analysis using the indicated strains are shown.

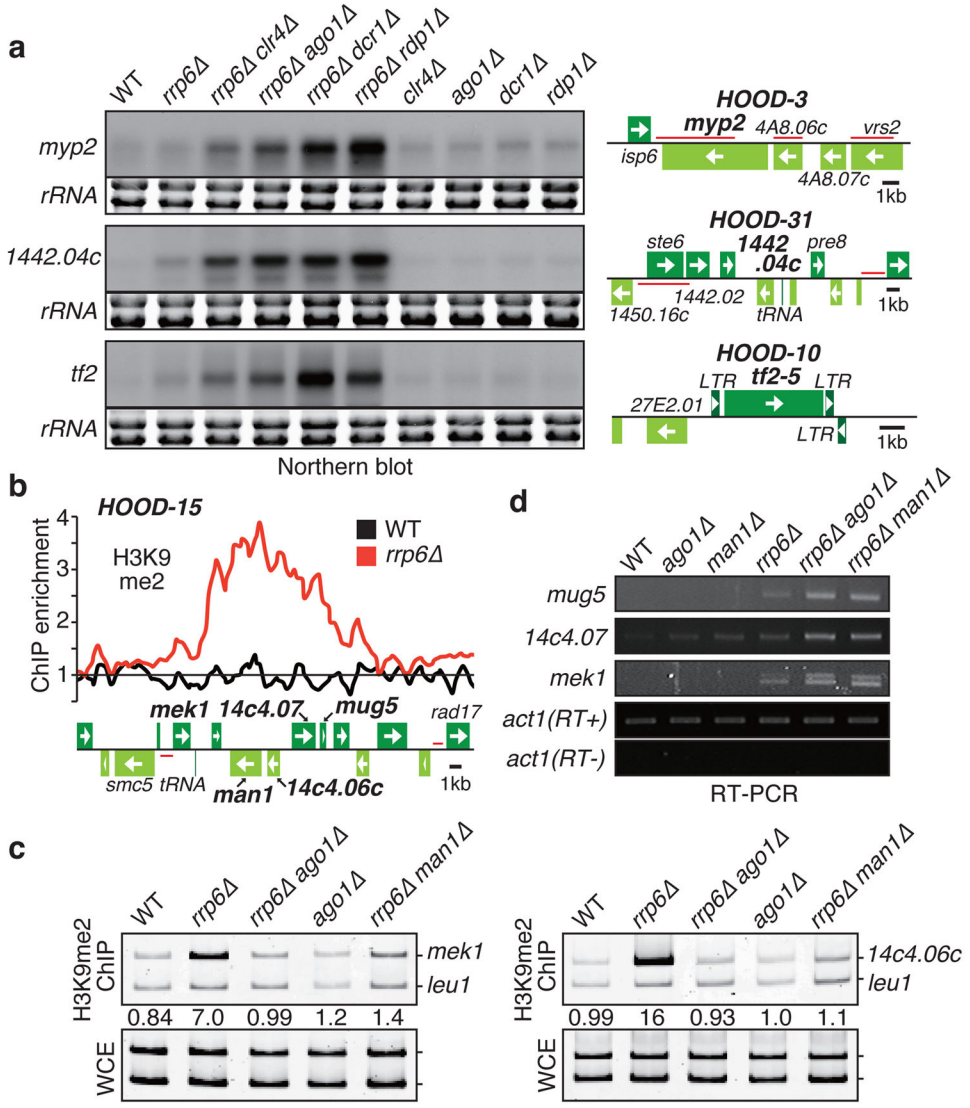

Figure 3. RNAi and heterochromatin factors acts in an overlapping manner with the exosome to silence genes located in HOODs

a, The role of Clr4 and RNAi in silencing *myp2*, *SPCC1442.04c*, and *Tf2* was analyzed by Northern analysis with a strand-specific probe to detect sense transcript. **b**, The H3K9me distribution across HOOD-15 as determined by ChIP-chip analysis of wild-type and *rrp6*Δ cells is shown. **c**, The effect of deleting the HOOD-15 *man1* gene, which contains a major siRNA cluster, on H3K9me at the nearby *mek1* and *SPAC14c4.06c* loci was determined by ChIP. **d**, The effect of *man1* on silencing of other genes in HOOD-15 was determined by strand-specific RT-PCR.

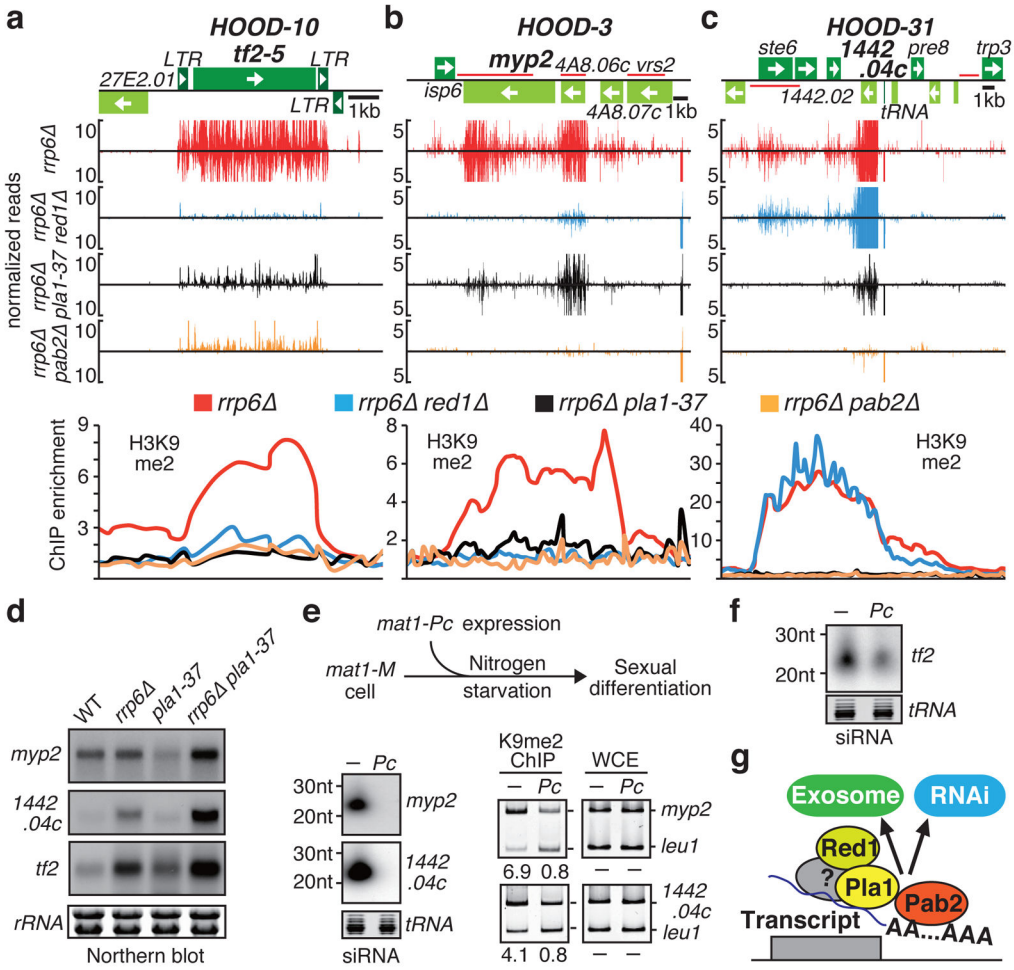

Figure 4. Specialized machinery triggers RNAi to regulate developmental genes and silence retroelements

a–c, Small RNA reads in the indicated strains are plotted along the genomic region of HOOD-10 (**a**) HOOD-3 (**b**), and HOOD-31 (**c**). Because *pla1* is essential, a partial loss of function *pla1-37* allele was used. H3K9me distribution was determined by ChIP-chip. **d**, Northern analysis of sense transcripts produced from *myp2*, *SPCC1442.04c* and *Tf2* loci in the indicated strains. **e**, Induction of sexual differentiation by ectopic expression of *mat1-Pc* in *mat1-M* cells under nitrogen starvation conditions was used to assay siRNA and H3K9me at the *myp2* and *SPCC1442.04c* loci. **f**, Detection of siRNAs mapping to *Tf2* under conditions that induce sexual differentiation. **g**, Schematic representation of the current model. Transcripts from sexual differentiation genes, genes containing transmembrane domains and retroelements are recognized by a mechanism involving Pla1, Red1 and Pab2, which promotes degradation of RNAs by RNAi and/or the exosome.